frontiers | Frontiers in Materials

Development and antioxidant evaluation of mango leaf (*Mangifera indica* L.) extract loaded silk fibroin nanoparticles

Nguyen Thi Ngoc Phuong[1], My Tien Ha[2],
Doan Xuan Tien Nguyen[2], Ngoc Yen Nguyen[2],
Huynh Anh Thi Huynh[2], Trieu Phu Hau[2], Tran Thi Bich Quyen[3],
Manh Quan Nguyen[4], Anh Tuan Nguyen[5] and Duy Toan Pham[2]*

[1]Faculty of Health Sciences, Dong Nai Technology University, Bien Hoa City, Vietnam, [2]Department of Health Sciences, College of Natural Sciences, Can Tho University, Can Tho, Vietnam, [3]Faculty of Chemical Engineering, College of Engineering, Can Tho University, Can Tho, Vietnam, [4]Department of Analytical Chemistry-Drug Quality Control, Faculty of Pharmacy, Can Tho University of Medicine and Pharmacy, Can Tho, Vietnam, [5]Department of Medicine and Pharmacy, Nam Sai Gon Polytechnic College, Ho Chi Minh City, Vietnam

The main antioxidant polyphenol compounds in the mango (*Mangifera indica* L.) leaf extract are susceptible to environmental degradations. Thus, in biomedical applications, the mango leaf extract is commonly encapsulated in a carrier. However, most studies employed the synthetic carrier materials that could affect the human health, and the complicated formulation procedure that could hinder the scalability. Therefore, this work, for the first time, explored the use of silk fibroin (an FDA-approved biomaterial), in nanoparticles platform, to encapsulate and deliver the mango leaf extract, utilizing the simple coacervation preparation method. Initially, the mango leaf ethanolic extract was obtained through maceration, resulting in a total phenolic content of 76.39 ± 0.14 mg GAE/g DPW and a notably high antioxidant activity ($IC_{50} = 6.872 \pm 0.512$ µg/mL). Subsequently, silk fibroin nanoparticles loaded with the extract were developed by the coacervation technique. Depending on the fibroin content, these nanoparticles exhibited an appropriate size range of 500−800 nm with narrow size distributions, a spherical shape with smooth surfaces, a dominant silk-II crystalline structure, a drug entrapment efficiency exceeding 70%, and retained the main biomarker mangiferin. Moreover, the phenolic-compounds release profiles from the particles followed the three-step process, the first burst-release step, the second sustained-release step, and the third degradation step. The particles were also non-toxic to the erythrocytes and the human embryonic kidney HEK-293 cell line. Lastly, the 2,2-diphenyl-1-picrylhydrazyl (DPPH) assay demonstrated that the antioxidant activity of the mango leaf extract was preserved within the extract-loaded nanoparticles. The results suggested that the silk fibroin nanoparticles could be a potential platform to effectively encapsulate and deliver the mango leaf extract for biomedical purposes.

KEYWORDS

silk, fibroin, nanoparticles, mango, Mangifera indica L, antioxidant

GRAPHICAL ABSTRACT
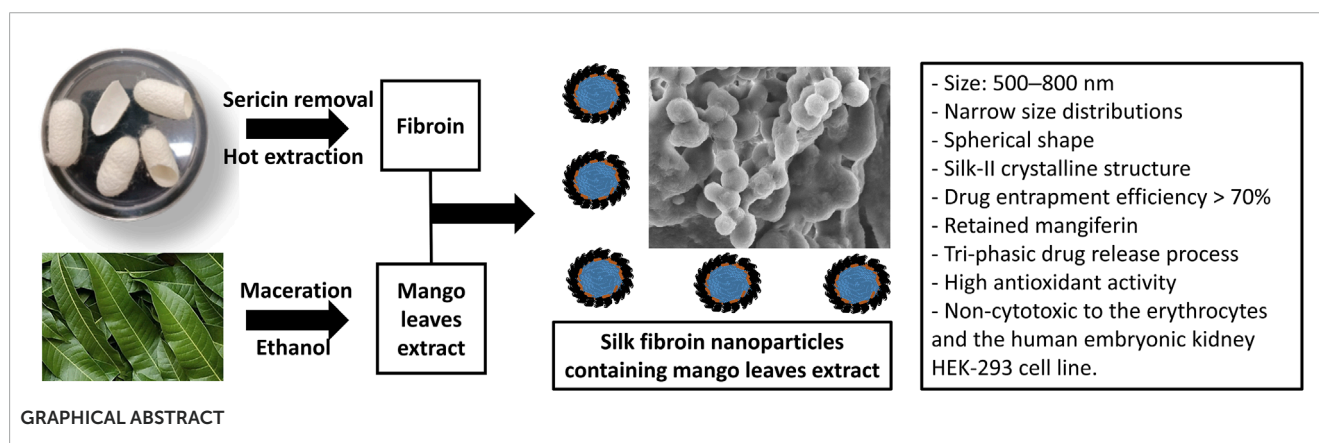
Highlights

- Novel mango-leaf ethanolic-extract loaded silk fibroin nanoparticles have been developed by simple coacervation method.
- The nanoparticles exhibited appropriate physicochemical properties and retained the main mango leaf biomarker mangiferin.
- The phenolic-compounds release profiles from the nanoparticles followed the three-step controllable process.
- The nanoparticles were non-toxic to the erythrocytes and the human embryonic kidney HEK-293 cell line.
- The nanoparticles significantly preserved the antioxidant activity of the mango leaf extract.

1 Introduction

Recently, silk fibroin emerges as a promising biomaterial designed as a delivery system for various medical applications (Mathur and Gupta, 2010; Pham and Tiyaboonchai, 2020). Derived from the cocoons of *Bombyx mori* silkworms, silk fibroin is a non-toxic-and-biodegradable natural protein that has been approved as a biological substance from the US Food and Drug Administration (FDA) (Chomchalao et al., 2020). Fibroin structure composes of a heavy chain and a light chain, with the respective molecular weight of ~390 kDa and ~26 kDa, connected to each other *via* a disulfide linkage; and a glycoprotein P25 bound to the chains (Pham and Tiyaboonchai, 2020). Regarding the amino acid composition, fibroin from *B. mori* silkworm generally contains glycine (43%), alanine (30%), and serine (12%) (Nguyen N. Y. et al., 2023). The exceptional stability of silk fibroin can be attributed to substantial hydrogen bonding, an amphiphilic nature, and a high degree of crystallinity (Pham et al., 2020a). With these potential properties, fibroin has been fabricated into numerous platforms, namely, microparticles (Baimark et al., 2010), hydrogel (Pham et al., 2022b), contact lenses (Jeencham et al., 2020), and especially, nanoparticles (Pham et al., 2019b). However, most studies focus on the delivery of synthetic pharmaceutical agents, with limited emphasis on the natural compounds and extracts.

Regarding this issue, silk fibroin nanoparticles (SFNs) have been successfully utilized as carriers for a few natural bioactive compounds (Lozano-Pérez et al., 2014; Lozano-Pérez et al., 2017; Pham et al., 2019a; Crivelli et al., 2019; Pham et al., 2020b; Pham et al., 2022a). Examples include alpha-mangostin for managing cancers (Pham et al., 2019a), resveratrol for treating intestinal inflammation (Lozano-Pérez et al., 2014), quercetin for antioxidant activity (Lozano-Pérez et al., 2017), and paclitaxel for cancer treatment (Pham et al., 2020b). For the natural plant extracts, to the best of our knowledge, only four articles on this issue have been published (as of 12/2023), in which the SFNs were used to deliver the olive leaf extract (Bayraktar et al., 2019), the guava leaf extract (Pham et al., 2023b), the rosemary extract (Hcini et al., 2021), and the wedelia extract (Pham et al., 2023a). These reports have demonstrated the outstanding SFNs properties in delivering the plant extracts, with adjustable particles sizes, high drug entrapment efficiencies, and controllable drug release rates. Hence, to further investigate the SFNs ability to encapsulate and deliver the natural plant extracts, this work was conducted, focused on the mango leaf ethanolic extract.

Mango (*Mangifera indica* L.) stands as a popular fruit and holds significant importance as a traditional medicine in the ASEAN region and various tropical and subtropical areas (Galán Saúco, 2004; Hirano et al., 2010). It is recognized as an excellent natural source of non-toxic antioxidants (Núñez Sellés et al., 2002). Extensive ethnopharmacological and clinical investigations have consistently highlighted the notable antioxidant capabilities of mango through both *in-vitro* and *in-vivo* research across diverse fields such as food, medicine, and cosmetics (Itoh et al., 2020; Molla et al., 2020). The mango leaf extract contains a high amount of polyphenols that possess significant antioxidant activity, including the well-known mangiferin (Kumar et al., 2021; Samanta et al., 2019). Mangiferin, also referred to as C-glucosyl xanthone, is functioning as a natural polyphenolic antioxidant within various parts of the mango tree, especially its leaves (Ebere Okwu and Ezenagu, 2008; D'zbreveamić et al., 2011). The biological activity of these phenolic compounds stems from the unsaturated bonds present in their chemical structures. However, the vulnerability of mango polyphenol molecules to environmental factors such as heat, light, pH, and enzymes is a noteworthy consideration (Saénz et al., 2009). Previous studies have reported the encapsulations of mango leaf extracts in Eudragit® L100 carrier using an electrospraying process (Sirirungsee et al., 2023), in porous ceramic matrices using supercritical CO_2 impregnation (Guamán-Balcázar et al.,

2022), and in lecithin-based emulsion using double emulsification method (Velderrain-Rodríguez et al., 2019). Nevertheless, the synthetic/metal-based carrier materials in these studies could possess human incompatibility/toxicity and might not suitable for biomedical applications (Nivetha et al., 2023). Moreover, these complicated formulating methods might hinder the scale-up processes in pilot and full-scale manufacturing production. Therefore, it is necessary to investigate novel biomaterials (i.e., fibroin) for mango leaf extract encapsulation, utilizing simple formulation technique (i.e., coacervation).

Ultimately, taken these aforementioned issues into consideration, this research, for the first time, aimed to create and thoroughly elucidate the capability of SFNs to encapsulate, deliver, and maintain the antioxidant activity of phenolic compounds extracted from mango leaf ethanolic extract. For this, the mango leaves were initially subjected to ethanol extraction using the maceration procedure, followed by the determination of their total phenolic content, and *in-vitro* antioxidant activity. Subsequently, the extract was incorporated into SFNs by a simple coacervation method, and the novel nanoparticles underwent assessment for sizes, shapes, structures, drug entrapment efficiency/loading capacity, drug release patterns, *in-vitro* cytotoxicity, and antioxidant activity.

2 Materials and methods

2.1 Materials

The fresh mango leaves (oblong shape, ~25-cm long and ~5-cm wide, dark green color on the upper surface and light green on the lower surface) were collected in Can Tho city, Vietnam, in 12/2022. The samples underwent identification based on morphological characteristics outlined in the book "Plants of Vietnam" (Hộ, 1999) and the corresponding voucher specimens were stored at the College of Natural Sciences, Can Tho University, Can Tho, Vietnam. The silkworm variety *B. mori* M45 was sourced from Nam Dinh province, Vietnam, *via* commercial business. Folin-Ciocalteu reagent, ascorbic acid (99%), and 2,2-Diphenyl-1-picrylhydrazyl (DPPH, 95%) were imported from Merck, Germany. Gallic acid (99.7%) and Na_2CO_3 (99.8%) were bought from Xilong, China. All other utilized chemicals were of reagent grades or higher.

2.2 Mango leaves extraction

The simple maceration technique was employed to extract the mango leaves. For this, the fresh mango leaves underwent air-drying at room temperature and were finely powdered. Subsequently, the powder was subjected to extraction using a 70% ethanol solution, with a weight-to-volume ratio of 1:20 (w/v), employing an ultrasound-assisted extraction method. After 20 min, the initial extract was collected, and the remaining solid residue underwent two additional extraction cycles. The resulting extracts (mango leaf ethanolic extract (MEE)) were then filtered, the solvent was evaporated using a rotavapor until a semi-solid consistency was achieved, and the extract was stored at 4°C for subsequent experiments.

To determine the total phenolic content in the MEE, the Folin-Ciocalteu method was employed, with slight modifications following the approach of Singleton and Rossi (Singleton and Rossi, 1965). To this end, 0.5 mL of the MEE was mixed with 2.5 mL Folin-Ciocalteu reagent and 2 mL 7.5% w/v Na_2CO_3 solution. After a 60-min incubation, the solution absorbance was measured at 765 nm using a UV-Vis spectrophotometer. The standard curve was established by varying gallic acid concentrations from 0 to 10 μg/mL, resulting in the equation y = 0.0874x + 0.0378 (R^2 = 0.9971). Eq. 1 was then utilized to compute the total phenolic content of MEE, expressed as mg gallic acid equivalent per gram of dry powder weight (mg GAE/g DPW).

$$Total\,phenolic\,content\,(mg\,GAE/g\,DPW) = \frac{C \times V \times k \times 10^3}{m} \times 100 \tag{1}$$

where C, V, k, and m is the phenolic concentrations in the test solution (μg/mL), the test solution volume (mL), the dilution factor, and the dry powder weight (mg).

2.3 Fibroin extraction

Fibroin extraction from silk cocoons was conducted through microwave-assisted heat extraction (Pham et al., 2018). Firstly, to remove sericin (the outer layer of silk fibers), 10 g of silk cocoons underwent treatment with a 0.5% w/v Na_2CO_3 solution at 100°C for 1 h. Subsequently, the resulting product was rinsed with distilled water and allowed to air-dry naturally. The sericin-removed silk was then dissolved in a $CaCl_2$:H_2O:$Ca(NO_3)_2$:EtOH solution (30:45:5:20 w/w/w/w), underwent heating in a microwave oven (900 W) for 2 min, followed by dialysis against distilled water for 3–5 days at room temperature using a cellulose dialysis bag (10000 MWCO). To eliminate impurities, the dialysis fluid was subjected to centrifugation at 10,000 rpm for 30 min at 4°C. Lastly, the silk fibroin solution was freeze-dried, and the fibroin powder was stored at 4°C for future research.

2.4 Blank SFNs and MEE-SFNs formulations

Prior to the fabrication of the MEE loaded SFNs (MEE-SFNs), the corresponding blank particles (i.e., unloaded SFNs) were prepared. For this, three blank SFN formulas were investigated, with initial fibroin concentrations of 1%, 2%, and 3% (w/v), respectively. The fibroin solutions were firstly reconstituted by dissolving the lyophilized fibroin powder in 5 mL water. Next, 2 mL fibroin solution was gently mixed with 1 mL 70% ethanol and agitated for 24 h at 4°C. Lastly, the spontaneously formed blank SFNs were centrifuged (6,000 rpm, 40 min) before being re-dispersed in water, freeze-dried, and kept at 4°C for the following tests (Pham et al., 2018).

The method for fabricating 03 MEE-SFNs formulas, correspond to fibroin concentrations of 1%/2%/3%, was similar to that for the blank SFNs. To this end, 1 mL of 70% ethanol was substituted with 1 mL of MEE (2.5 mg/mL total phenolic content). The formed MEE-SFNs were then centrifuged (6,000 rpm, 40 min), re-dispersed in water, freeze-dried, and kept at 4°C for the following tests.

2.5 Particles characterizations

The final products, SFNs and MEE-SFNs, were determined their 1) sizes and polydispersity indexes (PDI), 2) shape and morphology, 3) drug entrapment efficiency/loading capacity, and 4) chemical interactions.

Regarding the sizes and PDI, the freeze-dried SFNs and MEE-SFNs samples were re-dispersed in 2 mL water, homogenized, and measured with a Microtrac S3500 analyzer at 25°C using the dynamic light scattering (DLS) technique with standard parameters set by the instrument. The particles sizes and PDI were reported in terms of mean ± standard deviations (SD).

In terms of particles shape and morphology, the scanning electron microscopy (SEM) technique was employed. The freeze-dried particles were re-dispersed in 1 mL water and the dispersions were subjected onto the carbon-coated copper holder, following air-dried. Then, the samples were platinum coated and were SEM observed.

For the drug entrapment efficiency/loading capacity, the total phenolic content in the MEE-SFNs was determined utilizing the Folin-Ciocalteu reagent. For this, following the formation of MEE-SFNs, 0.5 mL of the supernatant of the centrifuge step was combined with 2.5 mL Folin-Ciocalteu reagent and 2 mL Na_2CO_3 solution (7.5% w/v), and incubated in the dark for 60 min. Then, the solution absorbance was UV-Vis spectroscopic determined at 765 nm and quantified using the calibration curve. Finally, Eqs 2, 3 were used to calculate the phenolic content entrapment efficiency and loading capacity, respectively.

$$Entrapment\,efficiency\,(\%)$$
$$= \frac{Amount\,of\,total\,phenolic\,content\,in\,SFNs}{The\,initial\,amount\,of\,total\,phenolic\,content\,in\,the\,MEE} \times 100\% \quad (2)$$

$$Drug\,loading\,capacity\,(\%)$$
$$= \frac{Amount\,of\,total\,phenolic\,content\,in\,SFNs}{The\,total\,amount\,of\,particles} \times 100\% \quad (3)$$

After loading SFNs with MEE, the Fourier-transform infrared spectroscopy (FTIR) was employed to detect the material structural alterations and chemical interactions. The spectra were captured with a JASCO-4600 machine with a spectral range of 4,000–400 cm^{-1}, a resolution of 1 cm^{-1}, and a triglycine sulfate detector. The freeze-dried SFNs and MEE-SFNs were mixed with dried KBr powder (ratio 1:10 w/w) and pressed under the pellet press to form thin tablets. The tablets were then subjected to FTIR measurements using the standard operational procedure.

2.6 Particles drug release evaluations

Regarding the drug release profile, the amount of total phenolic compounds released from the particles was evaluated using the shaker method at 37°C ± 0.5°C. In brief, 10 mg of the freeze-dried MEE-SFNs were distributed in 50 mL phosphate buffered saline (PBS, pH 7.4) and agitated at 200 rpm for 210 min. At each predetermined time intervals, 1 mL sample was extracted, buffer refilled, and centrifuged at 15,000 rpm for 5 min. The drug release in the supernatant was then reacted with Folin-Ciocalteu reagent and

UV-Vis spectroscopic evaluated at 765 nm. The cumulative phenolic release amounts were computed by Eq. 4.

$$Cumulative\,release\,(\%) = \frac{C_t V_0 + V\sum_1^{t-1} C_i}{M_0 - \sum_1^{t-1} M_i} \times 100\% \quad (4)$$

Where C_t, C_i are the concentrations of released total phenolic compounds at the time point t and i; V_0 is the total PBS volume (50 mL); V is the withdrawal sample volume (1 mL); M_0 is the initial amount of total phenolic content; and M_i is the total amount of drug withdrawal at the time point i.

2.7 Biomarker determination

To further confirm the incorporation of the phenolic compounds in the SFNs, especially the MEE main biomarker mangiferin, liquid chromatography-mass spectrometry (LC-MS/MS) technique was utilized. To this end, the freeze-dried MEE-SFNs were re-dispersed in 5 mL 70% ethanol, incubated at room temperature for 24 h to extract the MEE that was loaded into the particles. Next, the dispersions were centrifuged (15,000 rpm, 30 min) to remove the particles, and the supernatants were freeze-dried. The freeze-dried powder was then dissolved in methanol to concentration of 200 μg/L and subjected to LC-MS/MS analysis [ACQUITY UPLC H-CLASS SYSTEM Waters, Xevo TQD MS/MS (United States)] by positive electrospray ionization with capillary voltage of 4 kV and cone voltage of 30 V.

2.8 Particles cytotoxicity

The cytotoxicity of the SFNs and MEE-SFNs was assessed in both the red blood cells (i.e., hematotoxicity) and the normal human embryonic kidney HEK-293 (ATCC CRL-1573™) cell line.

For the hematotoxicity test, the sheep whole blood was obtained from Nam Khoa Limited Liability Company, Vietnam (ISO 13485, ISO 9001, and WHO GMP standards). The whole blood was centrifuged (4,000 rpm, 5 min) to get the red blood cells (i.e., the precipitate) and the cells were re-suspended in PBS to yield the final concentration of 1% w/v (1% hematocrit). Then, a fixed amount of the freeze-dried particles was re-dispersed in 1 mL of the prepared sheep red blood cells to get the final concentrations of 0.5, 1.25, 2.5, and 5 mg/mL. Next, the mixtures were incubated for 30 min at 37°C, centrifuged (4,000 rpm, 5 min), and the hemoglobin in the supernatant was UV-Vis spectroscopic quantified at 540 nm. The hematotoxicity of the particles were assessed by the percentages of hemolysis, calculated using Eq. 5. Water and PBS was used as the positive and negative controls, respectively.

$$Hemolysis\,(\%)$$
$$= \frac{Absorbance\,(test\,sample) - Absorbance\,(negative\,control)}{Absorbance\,(positive\,control) - Absorbance\,(negative\,control)}$$
$$\times 100\% \quad (5)$$

For the HEK-293 cytotoxic test, the standard (3-[4,5-dimethylthiazol-2-yl]-2,5 diphenyl tetrazolium bromide) (MTT) assay was employed. The cells were cultured in Dulbecco's modified

Eagle's medium (DMEM) supplemented with 10% fetal bovine serum and 1% PenStrep (penicillin and streptomycin). Prior to the experiments, the cells were seeded onto the 96-well plates (2×10^4 cells/well) and incubated at 37°C for 24 h. Then, 10 μL nanoparticles dispersions, at concentrations of 128, 32, 8, 2, and 0,5 μg/mL, were subjected to each well, followed by a 72-h incubation at 37°C. Next, the particles were withdrawn, the cells were washed with PBS, and 10 μL MTT solution (5 mg/mL) was added to each well. After another 4-h incubation, the formazan crystals (if any) were dissolved using 100 μL dimethylsulfoxide and the solutions were UV-Vis spectroscopic measured at 540 nm by a microplate reader. Cells treated with ellipticine (0.01 mM in dimethylsulfoxide), untreated cells, and the solvent without cells, was used as the positive control, the negative control, and the blank/background control, respectively. The percentages of cell viability were calculated by Eq. 6.

$$Cell\, viability\, (\%)$$
$$= \frac{Absorbance\, (test\, sample) - Absorbance\, (blank\, control)}{Absorbance\, (negative\, control) - Absorbance\, (blank\, control)}$$
$$x\, 100\% \qquad (6)$$

2.9 *In vitro* antioxidant activity

To evaluate the antioxidant activity of the MEE and the particles, the DPPH assay was utilized, following the standard method with some modification (Chandra Shekhar and Goyal, 2014; Sowmya et al., 2023). For the MEE, 960 μL of the extracts, at concentrations of 0, 2, 4, 6, 8, and 10 μg/mL, were mixed with 40 μL DPPH (1 mg/mL in methanol) and incubated in the dark at room temperature for 30 min. Then, the sample scavenging activities were UV-Vis spectroscopic determined at 517 nm, and calculated using Eq. 7. Lastly, the sample IC_{50} was derived accordingly based on the calibration curves. The negative control was DPPH + methanol and the reference was ascorbic acid.

$$DPPH\, scavenging\, effect\, (\%)$$
$$= \frac{Absorbance\, (negative\, control) - Absorbance\, (sample)}{Absorbance\, (negative\, control)}$$
$$x\, 100\% \qquad (7)$$

For the MEE-SFNs, 960 μL of the particles dispersions were combined with 40 μL DPPH (1 mg/mL in methanol) and incubated in the dark at room temperature for 30 min, 90 min, or 180 min. The samples were then centrifuged (2000 rpm, 2 min) to reduce the impact of SFNs on the measurements, and the supernatant was UV-Vis spectroscopic measured at 517 nm. The DPPH scavenging effect (%) of the particles was then determined based on Eq. 7.

2.10 Statistical analysis

All experiments were performed in triplicate and the data were described as mean ± SD. One-way analysis of variance (ANOVA) and Student's *t*-test were used for samples comparison, where necessary, with the *p*-value of <0.05 for significant differences.

3 Results and discussion

SFNs have been extensively employed as drug delivery systems in numerous biomedical settings. Nevertheless, limited information has been reported on the SFNs ability to deliver the whole plant extract. Thus, this research developed MEE loaded SFNs and characterized the products in terms of physicochemical properties, *in-vitro* hematotoxicity and cytotoxicity, and *in-vitro* antioxidant activity.

3.1 Mango leaves extraction

To extract the mango leaves, simple ultrasound-assisted maceration method was utilized, resulting in an extraction efficiency of 9.79% ± 0.92%. This result was lower than that of a published report, which showed that the extraction efficiency of the mango leaves from Da Nang (Vietnam) was 14.17% (Loan et al., 2021). The dark-greenish MEE extract had a moisture content of 7.22% ± 0.03%, which was suitable for further studies. MEE possessed a total phenolic content of 76.39 ± 0.14 mg GAE/g DPW, which was greater than that of the previous research (20.67 ± 0.07 mg GAE/g DPW) (Molla et al., 2020). These differences were attributed to changes in the bioactive chemicals content of mango leaves from different regions, cultivation duration, and soil and ambient conditions (Nguyen N. N. T. et al., 2023).

3.2 Blank SFNs and MEE-SFNs formulations and characterizations

The simple coacervation method was utilized for the formulations of SFNs and MEE-SFNs. This method involves the addition of coacervating agent (i.e., salt, a non-solvent, or a polymer) to a polymer solution, leading to a micro-environmental changes, consequently inducing the self-assembly formation of nanoparticles (Napiórkowska and Kurek, 2022). Compared to other common methods of electrospraying, supercritical CO_2 impregnation, and emulsification, the coacervation technique demonstrates various advantages of Eq. 1) high drug entrapment efficiency 2) ease of operation (i.e., low operational cost), with no requirement of advanced instruments and expertise, 3) versatility with the ability to encapsulate different compound types, 4) mild processing conditions with limited organic solvents (i.e., eco-friendliness), and 5) scalability (Jizomoto, 1984; Zhou et al., 2020; Napiórkowska and Kurek, 2022).

The SFNs and MEE-SFNs were formulated with varied initial fibroin concentrations of 1%, 2%, and 3%. For this, the particles hydrodynamic sizes, determined by the DLS measurements, were in the nano-range (~500 nm–~800 nm), with narrow size distributions (PDI <0.30) (Table 1). The initial fibroin concentrations significantly affected the particle sizes, as an increase in the fibroin concentrations yielded bigger particles. This could be due to the fact that fibroin is an amphiphilic polymer that undergoes self-assembly process during the coacervation process, forming additional intra-/intermolecular bonding, consequently resulting in SFNs (Pham et al., 2023c). Thus, as the amount of fibroin increases, more fibroin self-assembles simultaneously, making more interactions,

TABLE 1 Particles sizes and polydispersity indexes (PDI) of the blank SFNs and MEE-SFNs, at different fibroin concentration of 1%, 2%, and 3% ($n = 3$).

	Fibroin concentration (%)	Size (nm)	PDI
Blank SFNs	1	536 ± 32[a]	0.10 ± 0.02
	2	548 ± 28[a]	0.14 ± 0.04
	3	613 ± 14[b]	0.20 ± 0.03
MEE-SFNs	1	688 ± 16[c]	0.21 ± 0.03
	2	723 ± 11[d]	0.13 ± 0.03
	3	818 ± 35[e]	0.22 ± 0.02

* Different letters (a, b, c, d, e) denote significant differences ($p < 0.05$) between samples.

and enlarging the particles size. Moreover, the MEE-SFNs sizes were significantly bigger than those of the blank SFNs, indicating the incorporation of MEE affected the particle characteristics. Generally, the encapsulations of small molecular drugs in SFNs does not alter the particles sizes, since the drug molecules could bind non-covalently with the fibroin molecules in the particle pores (Pham et al., 2019a). However, in this case, the whole plant extract (i.e., MEE) was loaded into the particles. As the extracts possess several chemical compounds, more interactions were formed, which interfered with the fibroin intra-/intermolecular bonding, resulting in the bigger particles.

Regarding the particle shape, both the SFNs and MEE-SFNs demonstrated spherical shape with smooth surfaces (SEM micrograph, Figure 1). Some particles aggregations were also observed, which was in agreement with the previous studies on natural-extract loaded SFNs (Pham et al., 2023a; Pham et al., 2023b). Additionally, no significant difference was noted between the blank SFNs and the MEE-SFNs, suggesting the extract incorporating process did not affect the particle shape and morphology.

In terms of the entrapment efficiency and the loading capacity of the loading drug (i.e., the total phenolic content in the MEE), the particles with fibroin concentration of 1%, 2%, and 3% yielded the increasing entrapment efficiency of 77.965% ± 1.135%, 84.080% ± 2.034%, and 90.165% ± 1.012%, respectively; and the decreasing loading capacity of 8.880% ± 0.118%, 4.992% ± 0.115%, and 3.621% ± 0.039%, respectively. This indicated that the initial fibroin concentrations could alter the drug encapsulation processes. Since the phenolic compounds in the MEE interacts with fibroin molecules in the SFNs *via* the weak interactions such as hydrogen bonding and van der Waals forces, an increase in the fibroin amount resulted in more effective interactions, consequently enhances the drug entrapment efficiency. Nevertheless, when compared to the total particle mass, the loading capacity decreased, which stated that the particles have reached their saturation point (i.e., the point of which the fibroin and drug molecules have fully interacted) at high concentrations (Pham et al., 2020b).

For the chemical interactions, the FTIR spectra are presented (Figure 2). Both the blank SFNs and the MEE-SFNs possessed

characterized fibroin silk-II-crystalline peaks at 1,620–1,630 cm^{-1} and 1,515–1,522 cm^{-1}, corresponding to the amide C=O stretching and N-H bending areas, respectively (Pham et al., 2018). This shows that the raw fibroin silk-I amorphous structure was converted to silk-II crystalline structure throughout the formulation process (Hu et al., 2006; Zhang et al., 2006; Lozano-Pérez et al., 2014; Pham et al., 2018). During that process, by utilizing intra-/intermolecular hydrogen bonding (mostly between glycine and alanine) and van der Waals forces, the heavy chain can form stable anti-parallel β-sheet crystallites, changing the silk-I structure to silk-II structure. Additionally, the MEE-SFNs revealed the main phenolic peaks of the MEE, including the broad bands in the region 3,200–3,600 cm^{-1}, attributing to the presence of the phenolic O-H groups, and the peaks at 950–1,150 cm^{-1}, corresponding to the C-O stretching of the primary/secondary alcohol (Barnabas et al., 2022). These data demonstrate that the MEE was successfully encapsulated in the SFNs and the encapsulation process did not significantly alter the MEE or SFNs structures.

To further confirm the presence of the main MEE phenolic compound biomarker, mangiferin, in the particles, LC-MS/MS analysis was conducted. The spectra of all MEE-SFNs formulas gave an [M + H]$^+$ ion at m/z 423.2 (Figure 3), in accordance with the reported data of the standard mangiferin (2-β-D-glucopyranosyl-1,3,6,7-tetrahydroxy-9H-xanthen-9-one), a major antioxidant component of mango leaves (Prommajak et al., 2014; Jhaumeer Laulloo et al., 2018). Therefore, all particles could encapsulate the main MEE biomarker, mangiferin.

3.3 Drug release profiles from MEE-SFNs

Regarding the phenolic-compound release profiles of the MEE-SFNs, Figure 4 shows that the release process followed three steps, the first burst-release step from 0 to 30 min, the sustained-release step from 30 to 90 min, and the degradation step from 90 to 210 min. Since fibroin is an amphiphilic molecule, the SFNs self-positioned their hydrophilic domains on the particle surfaces (i.e., the side that contact water) and their hydrophobic domains on the interior (Pham et al., 2018). Thus, initially, the hydrophilic phenolic compounds located on the particles surfaces were rapidly released (19.15%, 23.72%, and 26.75% at fibroin concentration of 1%, 2%, and 3%). Then, for the next 60 min, the hydrophobic phenolic compounds that located inside the particles, with strong hydrophobic interactions with fibroin (Hu et al., 2006; Lozano-Pérez et al., 2017), were slowly released and reached their saturation points. Finally, for the remaining testing duration, the released compounds were degraded, consequently reduced the total phenolic contents. This behavior was consistent with a previous studies (Lozano-Pérez et al., 2017; Pham et al., 2023a; Pham et al., 2023b). Notably, the initial fibroin concentrations statistically affected the drug release rates, as the release amount increased with the fibroin concentration (i.e., 3% > 2% > 1%). This fact corresponds well with the percentages of drug entrapment efficiencies, suggesting particles with higher drug encapsulations demonstrate higher release amounts.
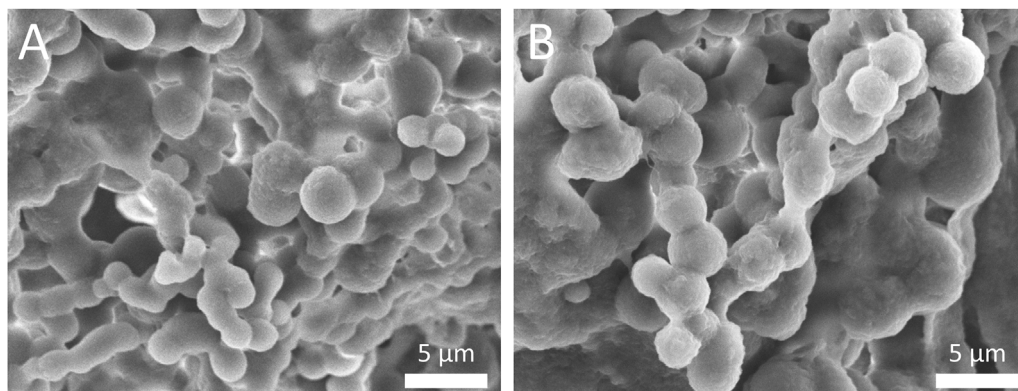
FIGURE 1
Scanning electron microscopy (SEM) micrographs of **(A)** blank SFNs and **(B)** MEE-SFNs. Scale bar: 5 μm. The particles demonstrated spherical shape and smooth surfaces with aggregation pattern.
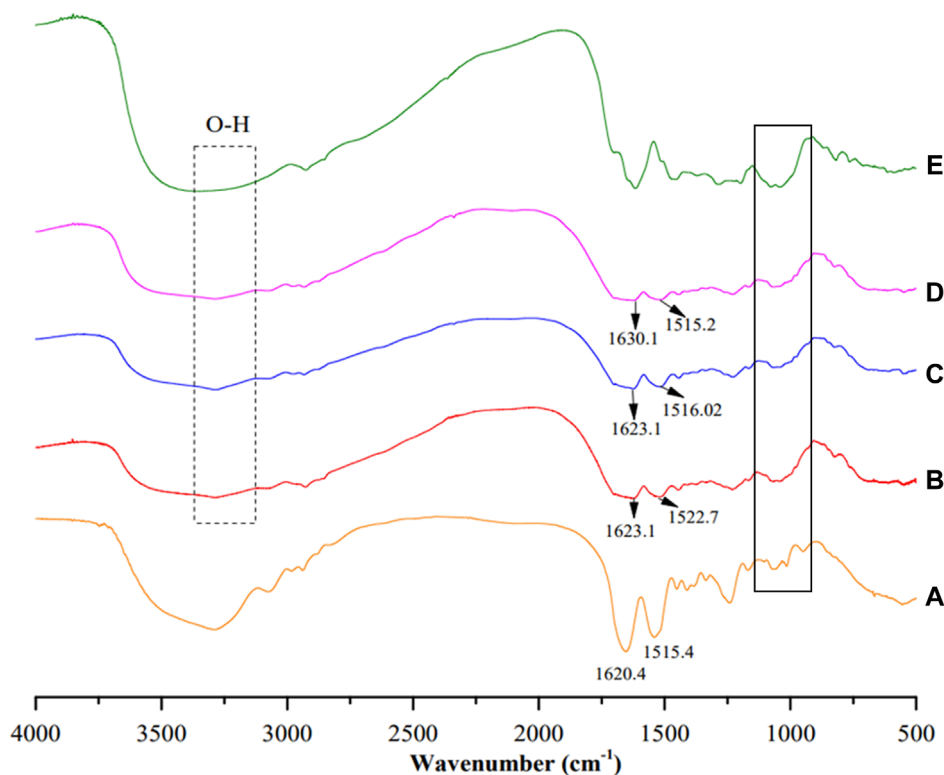

FIGURE 2
Fourier-transform infrared spectroscopy (FTIR) spectra of **(A)** blank SFNs, **(B)** MEE-SFNs-1% fibroin, **(C)** MEE-SFNs-2% fibroin, **(D)** MEE-SFNs-3% fibroin, and **(E)** Mango leaf ethanolic extract. The spectra demonstrated the fibroin and/or MEE characterized peaks.

3.4 Particles cytotoxicity

Fibroin has been approved by the FDA as a biomaterial with non-toxic biodegradable products (Pham and Tiyaboonchai, 2020). Nevertheless, during the formulation process and the incorporation of MEE, this non-toxic property might be altered. Thus, we conducted the cytotoxicity tests of the SFNs and MEE-SFNs on two representative cells, the red blood cells (erythrocytes) and the human embryonic kidney HEK-293 cell line. Erythrocytes are the main cell component in the human blood, attributing to 40%–45% of the blood volume, with the main function of supplying oxygen and nutrients for the body tissues (Barbalato and Pillarisetty, 2024). Acute hemolysis (i.e., the destruction of erythrocytes) could cause anemia and other severe complications (Baldwin et al., 2024). Thus, it is crucial to assess the cytotoxicity of the particles on the erythrocytes. Similarly, the HEK-293 cell line, derived from
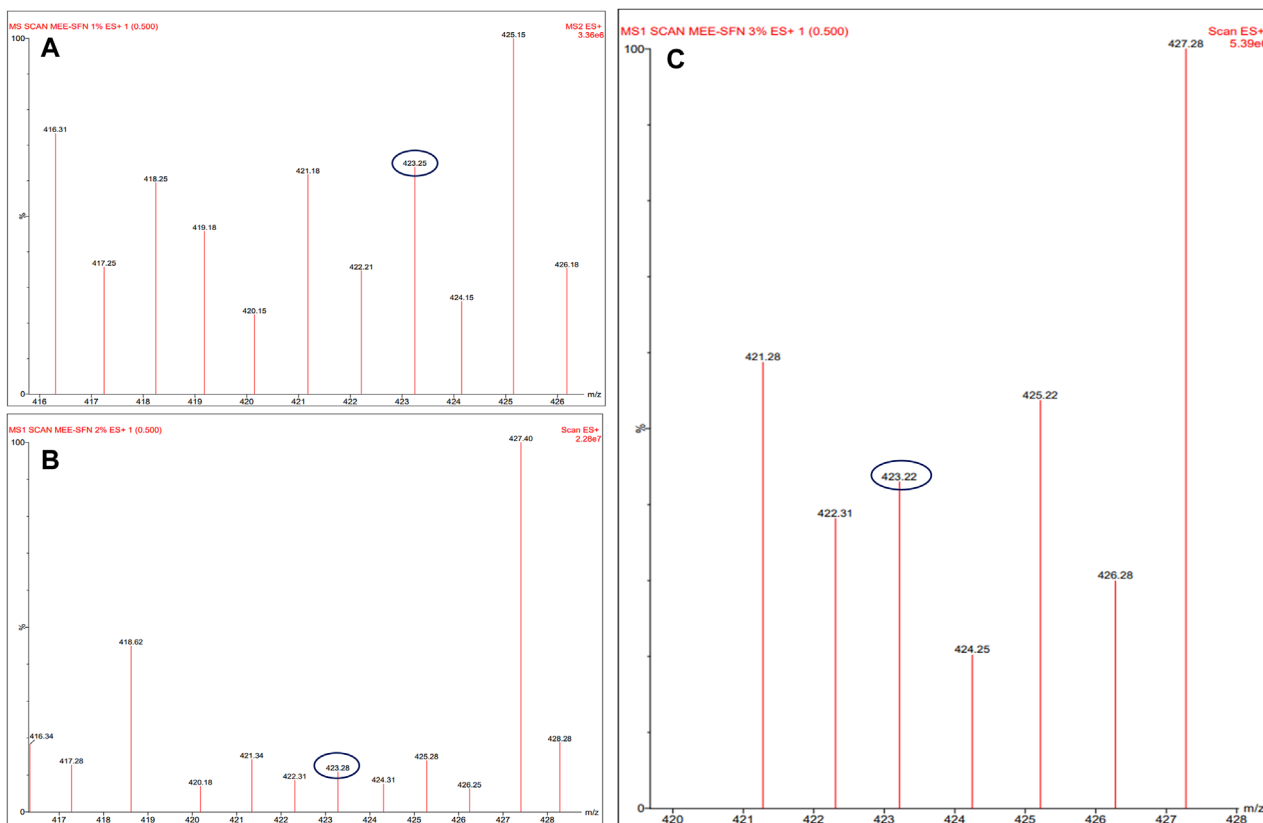
FIGURE 3
Liquid chromatography-mass spectrometry (LC-MS/MS) analysis of **(A)** MEE-SFNs-1% fibroin, **(B)** MEE-SFNs-2% fibroin, and **(C)** MEE-SFNs-3% fibroin. The MS revealed the signal of the main biomarker mangiferin.
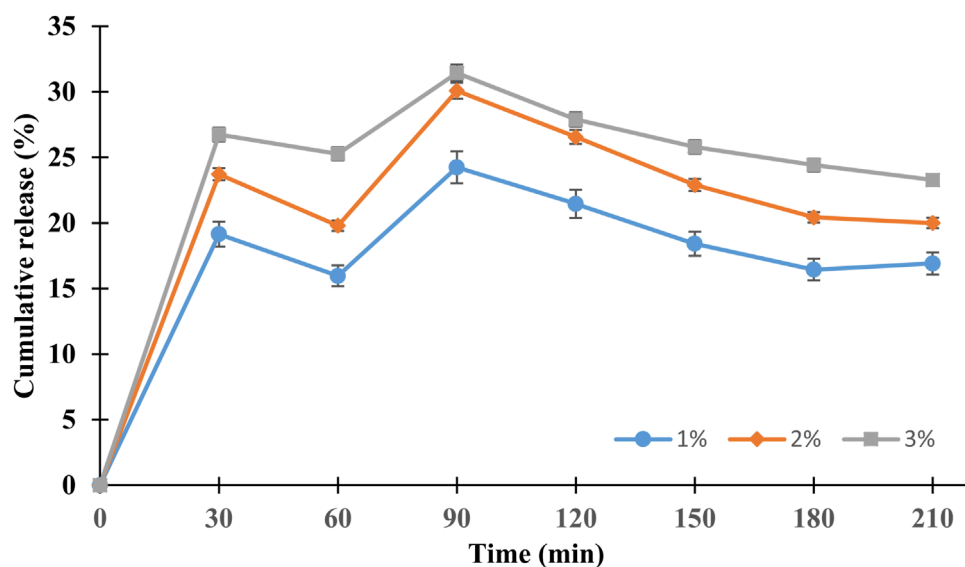

FIGURE 4
Phenolic compound release profiles of the MEE-SFNs (at different fibroin concentrations of 1%, 2%, and 3%) in PBS at pH 7.4 ($n = 3$). The release followed the three-step controllable process.
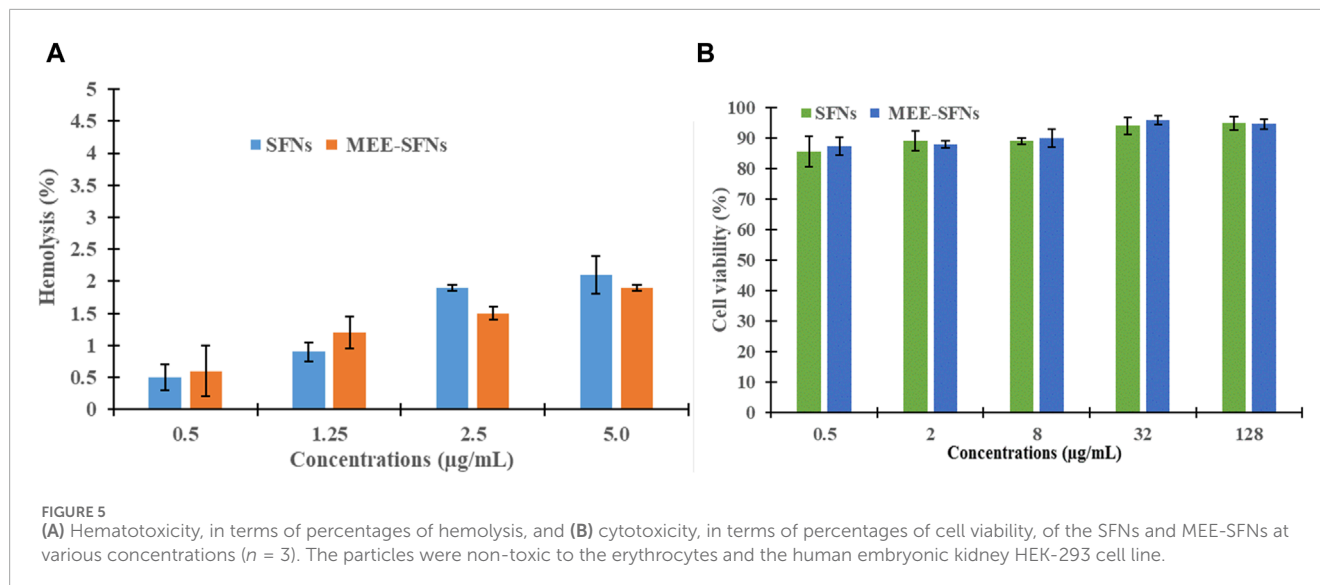
FIGURE 5
(A) Hematotoxicity, in terms of percentages of hemolysis, and **(B)** cytotoxicity, in terms of percentages of cell viability, of the SFNs and MEE-SFNs at various concentrations (n = 3). The particles were non-toxic to the erythrocytes and the human embryonic kidney HEK-293 cell line.

TABLE 2 The DPPH scavenging activity (%) of the MEE, the blank SFNs, and the MEE-SFNs at different fibroin concentration of 1%, 2%, and 3%, at various testing duration of 30 min, 90 min, and 180 min (n = 3).

	Fibroin concentration (%)	DPPH scavenging activity (%)		
		30 min	90 min	180 min
Blank SFNs	1	$5.252 \pm 0.425^{a, *}$	$5.263 \pm 0.523^{a, *}$	$5.616 \pm 0.431^{a, *}$
	2	$4.077 \pm 0.342^{b, *}$	$4.930 \pm 0.434^{a\#}$	$5.148 \pm 0.353^{a\#}$
	3	$4.503 \pm 0.329^{a, *}$	$4.758 \pm 0.312^{a, *}$	$5.159 \pm 0.544^{a, *}$
MEE-SFNs	1	$27.187 \pm 0.409^{c, *}$	$39.719 \pm 0.334^{b\#}$	$51.794 \pm 0.318^{b\$}$
	2	$30.754 \pm 0.532^{d, *}$	$42.215 \pm 0.229^{c\#}$	$53.313 \pm 0.532^{c\$}$
	3	$32.137 \pm 0.381^{e, *}$	$50.816 \pm 0.242^{d\#}$	$66.947 \pm 0.237^{d\$}$
MEE		$70.401 \pm 0.620^{f, *}$	$71.623 \pm 0.575^{e, *}$	$70.849 \pm 0.774^{e, *}$

*Different letters (a, b, c, d, e) denote significant differences ($p < 0.05$) between samples in the same column; different symbols (∗, #, $) denote significant differences ($p < 0.05$) between samples in the same row.

human embryonic kidney cells, is commonly used to determine the extracts/compounds nephro-cytotoxicity (Amalia et al., 2021).

All particles possessed a percentage of hemolysis of <5%, indicating the non-hematotoxicity property (Figure 5A) (Pham et al., 2020b; Nguyen N. Y. et al., 2023). Likewise, in the HEK-293 cell line, the particles showed a cell viability of >80% at concentrations of up to 128 µg/mL, equivalent to the total phenolic content (Figure 5B), suggesting that they were non-toxic to the normal HEK-293 cell, according to the standard grading systems of ISO 10993–5:2009 (Pham et al., 2019b). This could be because fibroin is biocompatible with the human system (Vepari and Kaplan, 2007) and MEE has been proven to be non-toxic in various cell lines (Ganogpichayagrai et al., 2017). Conclusively, the SFNs and MEE-SFNs could be considered safe in biological systems and the formulation process did not significantly alter the fibroin and MEE toxicological properties.

3.5 *In vitro* antioxidant DPPH assay

To confirm the antioxidant activity of the MEE itself and the MEE-SFNs, the standard DPPH scavenging assay was employed (Table 2). Firstly, the MEE activity was assessed, which resulted in an IC_{50} of 6.872 ± 0.512 µg/mL, comparable to that of ascorbic acid (vitamin C), with IC_{50} of 4.109 ± 0.551 µg/mL. Our extract was more active than that reported by Itoh et al. (2020), which revealed an IC_{50} value of 9 µg/mL (Itoh et al., 2020), which could be due to the various soil and ambient conditions in each region, resulting in different biological activities (Bafna and Balaraman, 2005; D'zbreveamić et al., 2011). Secondly, the capacity of the blank SFNs to scavenge DPPH free radicals was then tested. The results showed that all formulas had a modest radical scavenging activity of ~5%, probably due the presence of tyrosine residues in the silk fibroin sequences. Finally, the MEE-SFNs could effectively

retain the antioxidant efficacy of the encapsulated MEE, and the activity was time-dependent and concentration-dependent. For instance, the higher the fibroin concentration (i.e., higher drug entrapment efficiency) and the longer the incubation time (i.e., higher drug release amount), the better the antioxidant activity. The findings suggest that the antioxidant activity of MEE-SFNs was dependent on the release of phenolic chemicals from the particles, allowing for additional research into drug release control for the most effective action at the target.

4 Conclusion

This present study, for the first time, successfully encapsulated the mango leaf extract in a biomaterial carrier, silk fibroin nanoparticles, that is biocompatible with the human health, utilizing the simple formulation procedure of coacervation. The novel mango-leaf-ethanolic-extract loaded silk fibroin nanoparticles were physicochemical characterized, *in-vitro* cytotoxicity evaluated, and antioxidant-activity measured. The particles possessed appropriate properties as a drug delivery system, with mean sizes of 500–800 nm, narrow size distributions, spherical shapes, silk-II structures, high drug entrapment efficiencies of >70%, three-phase release profiles, and non-toxicity to the erythrocytes and the human embryonic kidney HEK-293 cell line. The particles also retained the antioxidant activity of the extract in a time-/concentration-dependent manner. Although demonstrating much potentials, the study limitation was that it was conducted in *in-vitro* settings, with no information on *in-vivo* experiments. This challenge could be overcome in the future research on animal models. Moreover, the scalability issue, as well as other activities of the product (i.e., antibacterial action), should be focused. In summary, proven by the case of mango leaf extract, the fibroin nanoparticles could be further utilized for delivering natural extracts to potentially become novel pharmaceutical/cosmeceutical products in the future.

Data availability statement

The original contributions presented in the study are included in the article/supplementary material, further inquiries can be directed to the corresponding author.

Author contributions

NTNP: Conceptualization, Data curation, Investigation, Methodology, Writing–original draft, Writing–review and editing.

MTH: Investigation, Methodology, Writing–review and editing. DXTN: Investigation, Methodology, Writing–review and editing. NYN: Investigation, Methodology, Writing–review and editing. HATH: Investigation, Methodology, Writing–review and editing. TPH: Investigation, Methodology, Writing–review and editing. TTBQ: Investigation, Methodology, Writing–review and editing. MQN: Investigation, Methodology, Writing–review and editing. ATN: Investigation, Methodology, Writing–review and editing. DTP: Conceptualization, Data curation, Methodology, Project administration, Resources, Validation, Writing–original draft, Writing–review and editing.

Funding

Acknowledgments

Conflict of interest

The authors declare that the research was conducted in the absence of any commercial or financial relationships that could be construed as a potential conflict of interest.

Publisher's note

All claims expressed in this article are solely those of the authors and do not necessarily represent those of their affiliated organizations, or those of the publisher, the editors and the reviewers. Any product that may be evaluated in this article, or claim that may be made by its manufacturer, is not guaranteed or endorsed by the publisher.

References

Amalia, R., Aulifa, D. L., Zain, D. N., Pebiansyah, A., and Levita, J. (2021). The cytotoxicity and nephroprotective activity of the ethanol extracts of *Angelica keiskei* Koidzumi stems and leaves against the NAPQI-induced human embryonic kidney (HEK293) cell line. *Evidence-Based Complementary Altern. Med.* 2021, 1–6. doi:10.1155/2021/6458265

Bafna, P. A., and Balaraman, R. (2005). Antioxidant activity of DHC-1, an herbal formulation, in experimentally-induced cardiac and renal damage. *Phytotherapy Res. PTR* 19, 216–221. doi:10.1002/PTR.1659

Baimark, Y., Srihanam, P., Srisuwan, Y., and Phinyocheep, P. (2010). Preparation of porous silk fibroin microparticles by a water-in-oil emulsification-diffusion method. *J. Appl. Polym. Sci.* 118, 1127–1133. doi:10.1002/app.32506

Baldwin, C., Pandey, J., and Olarewaju, O. (2024). "Hemolytic anemia," in *StatPearls* (Treasure Island (FL): StatPearls Publishing). Available at: http://www.ncbi.nlm.nih.gov/books/NBK558904/ (Accessed May 14, 2024).

Barbalato, L., and Pillarisetty, L. S. (2024). "Histology, red blood cell," in *StatPearls* (Treasure Island (FL): StatPearls Publishing). Available at: http://www.ncbi.nlm.nih.gov/books/NBK539702/(Accessed May 14, 2024).

Barnabas, H. L., Aliyu, B. A., Gidigbi, J. A., Abubakar, A. B., and Markus, A. (2022). Comparative analysis of stable aqueous dispersion of silver nanoparticle synthesized from Mangifera indica and azadirachta indica leaf extract. *NanoNEXT* 3, 1–10. doi:10.54392/NNXT2241

Bayraktar, O., Köse, M., and Baspinar, Y. (2019). Development of olive leaf extract loaded fibroin microparticles by spray drying. *Drug Discov.* 13, 39–45.

Chandra Shekhar, T., and Goyal, A. (2014). Antioxidant activity by DPPH radical scavenging method of Ageratum conyzoides. *Orient* 1, 244–249.

Chomchalao, P., Nimtrakul, P., Pham, D. T., and Tiyaboonchai, W. (2020). Development of amphotericin B-loaded fibroin nanoparticles: a novel approach for topical ocular application. *J. Mater. Sci.* 55, 5268–5279. doi:10.1007/S10853-020-04350-X

Crivelli, B., Bari, E., Perteghella, S., Catenacci, L., Sorrenti, M., Mocchi, M., et al. (2019). Silk fibroin nanoparticles for celecoxib and curcumin delivery: ROS-scavenging and anti-inflammatory activities in an *in vitro* model of osteoarthritis. *Eur. J. Pharm. Biopharm. official J. Arbeitsgemeinschaft fur Pharmazeutische Verfahrenstechnik e.V* 137, 37–45. doi:10.1016/J.EJPB.2019.02.008

D'zbreveamić, A. M., Marin, P. D., Gbolade, A. A., and Ristić, M. S. (2011). Chemical composition of *Mangifera indica* essential oil from Nigeria. *J. Essent. Oil Res.* 22, 123–125. doi:10.1080/10412905.2010.9700279

Ebere Okwu, D., and Ezenagu, V. (2008). Evaluation of the phytochemical composition of mango (Mangifera indica Linn) stem bark and leaves. *Int. J. Chem. Sci.* 6, 705–716.

Galán Saúco, V. (2004). Mango production and world market: current situation and future prospects. *Acta Hortic.*, 107–116. doi:10.17660/ACTAHORTIC.2004.645.7

Ganogpichayagrai, A., Palanuvej, C., and Ruangrungsi, N. (2017). Antidiabetic and anticancer activities of Mangifera indica cv. Okrong leaves. *J. Adv. Pharm. Technol. Res.* 8, 19–24. doi:10.4103/2231-4040.197371

Guamán-Balcázar, M. C., Montes, A., Valor, D., Coronel, Y., De los Santos, D. M., Pereyra, C., et al. (2022). Inclusion of natural antioxidants of mango leaves in porous ceramic matrices by supercritical CO_2 impregnation. *Mater. (Basel)* 15, 5934. doi:10.3390/ma15175934

Hcini, K., Lozano-Pérez, A. A., Cenis, J. L., Quílez, M., and Jordán, M. J. (2021). Extraction and encapsulation of phenolic compounds of Tunisian rosemary (*Rosmarinus officinalis* L.) extracts in silk fibroin nanoparticles. *Plants (Basel, Switzerland)* 10, 2312. doi:10.3390/PLANTS10112312

Hirano, R., Oo, T. H., and Watanabe, K. N. (2010). Myanmar mango landraces reveal genetic uniqueness over common cultivars from Florida, India, and Southeast Asia. *Genome* 53, 321–330. doi:10.1139/G10-005

Hộ, P. H. (1999). *Cây cỏ Việt Nam Nhà xuất bản trẻ*, 1–1027.

Hu, X., Kaplan, D., and Cebe, P. (2006). Determining beta-sheet crystallinity in fibrous proteins by thermal analysis and infrared spectroscopy. *Macromolecules* 39, 6161–6170. doi:10.1021/MA0610109

Itoh, K., Matsukawa, T., Okamoto, M., Minami, K., Tomohiro, N., Shimizu, K., et al. (2020). *In vitro* antioxidant activity of *Mangifera indica* leaf extracts. *J. Plant Stud.* 9, 39. doi:10.5539/JPS.V9N2P39

Jeencham, R., Sutheerawattananonda, M., Rungchang, S., and Tiyaboonchai, W. (2020). Novel daily disposable therapeutic contact lenses based on chitosan and regenerated silk fibroin for the ophthalmic delivery of diclofenac sodium. *Drug Deliv.* 27, 782–790. doi:10.1080/10717544.2020.1765432

Jhaumeer Laulloo, S., Bhowon, M. G., Soyfoo, S., and Chua, L. S. (2018). Nutritional and biological evaluation of leaves of Mangifera indica from Mauritius. *J. Chem.* 2018, 1–9. doi:10.1155/2018/6869294

Jizomoto, H. (1984). Phase separation induced in gelatin-base coacervation systems by addition of water-soluble nonionic polymers I: microencapsulation. *J. Pharm. Sci.* 73, 879–882. doi:10.1002/jps.2600730705

Kumar, M., Saurabh, V., Tomar, M., Hasan, M., Changan, S., Sasi, M., et al. (2021). Mango (*Mangifera indica* L.) leaves: nutritional composition, phytochemical profile, and health-promoting bioactivities. *Antioxidants (Basel, Switzerland)* 10, 299–323. doi:10.3390/ANTIOX10020299

Loan, N. T. T., Long, D. T., Yen, P. N. D., Hanh, T. T. M., Pham, T. N., and Pham, D. T. N. (2021). Purification process of mangiferin from Mangifera indica L. Leaves and evaluation of its bioactivities. *Processes* 9, 852. doi:10.3390/pr9050852

Lozano-Pérez, A. A., Rivero, H. C., Pérez Hernández, M. C., Pagán, A., Montalbán, M. G., Víllora, G., et al. (2017). Silk fibroin nanoparticles: efficient vehicles for the natural antioxidant quercetin. *Int. J. Pharm.* 518, 11–19. doi:10.1016/j.ijpharm.2016.12.046

Lozano-Pérez, A. A., Rodriguez-Nogales, A., Ortiz-Cullera, V., Algieri, F., Garrido-Mesa, J., Zorrilla, P., et al. (2014). Silk fibroin nanoparticles constitute a vector for controlled release of resveratrol in an experimental model of inflammatory bowel disease in rats. *Int. J. Nanomedicine* 9, 4507–4520. doi:10.2147/IJN.S68526

Mathur, A. B., and Gupta, V. (2010). Silk fibroin-derived nanoparticles for biomedical applications. *Nanomedicine.* 5, 807–820. doi:10.2217/nnm.10.51

Molla, M. M., Sabuz, A. A., Chowdhury, M. G. F., Khan, M. H. H., Alam, M., Miaruddin, M., et al. (2020). Nutritional composition, antioxidant activity and common phytochemicals of selected BARI mango varieties and commercial cultivar langra: phytochemical and antioxidant activities of BARI mango varieties. *Eur. J. Agric. Food Sci.* 2. doi:10.24018/EJFOOD.2020.2.6.151

Napiórkowska, A., and Kurek, M. (2022). Coacervation as a novel method of microencapsulation of essential oils—a review. *Molecules* 27, 5142. doi:10.3390/molecules27165142

Nguyen, N. N. T., Duong, X. C., Nguyen, K. N., Nguyen, T. N. V., Nguyen, T. T. D., Le, T. T. Y., et al. (2023a). Development and *in-vitro/in-vivo* evaluation of film-coated tablets containing Azadirachta indica A. Juss leaf extracts for diabetes treatment. *J. Appl. Pharm. Sci.* 13, 193–200. doi:10.7324/JAPS.2023.130119

Nguyen, N. Y., Nguyen, T. N. P., Huyen, N. N., Tran, V. D., Quyen, T. T. B., Luong, H. V. T., et al. (2023b). Onto the differences in formulating micro-/nanoparticulate drug delivery system from Thai silk and Vietnamese silk: a critical comparison. *Heliyon* 9, e16966. doi:10.1016/J.HELIYON.2023.E16966

Nivetha, N., Srivarshine, B., Sowmya, B., Rajendiran, M., Saravanan, P., Rajeshkannan, R., et al. (2023). A comprehensive review on bio-stimulation and bio-enhancement towards remediation of heavy metals degeneration. *Chemosphere* 312, 137099. doi:10.1016/j.chemosphere.2022.137099

Núñez Sellés, A. J., Vélez Castro, H. T., Agüero-Agüero, J., González-González, J., Naddeo, F., De Simone, F., et al. (2002). Isolation and quantitative analysis of phenolic antioxidants, free sugars, and polyols from mango (*Mangifera indica* L.) stem bark aqueous decoction used in Cuba as a nutritional supplement. *J. Agric. Food Chem.* 50, 762–766. doi:10.1021/jf011064b

Pham, D. T., Ha, T. K. Q., Nguyen, M. Q., Tran, V. D., Nguyen, V. B., and Quyen, T. T. B. (2022a). Silk fibroin nanoparticles as a versatile oral delivery system for drugs of different biopharmaceutics classification system (BCS) classes: a comprehensive comparison. *J. Mater. Res.* 37, 4169–4181. doi:10.1557/S43578-022-00782-0

Pham, D. T., Huynh, Q. C., Lieu, R., Nguyen, V. B., De Tran, V., Thi, B., et al. (2023a). Controlled-release wedelia trilobata L. Flower extract loaded fibroin microparticles as potential anti-aging preparations for cosmetic trade commercialization. *Clin. Cosmet. Investigational Dermatology* 16, 1109–1121. doi:10.2147/CCID.S405464

Pham, D. T., Nguyen, D. X. T., Lieu, R., Huynh, Q. C., Nguyen, N. Y., Quyen, T. T. B., et al. (2023b). Silk nanoparticles for the protection and delivery of guava leaf (Psidium guajava L.) extract for cosmetic industry, a new approach for an old herb. *Drug Deliv.* 30, 2168793. doi:10.1080/10717544.2023.2168793

Pham, D. T., Nguyen, T. L., Nguyen, T. T. L., Nguyen, T. T. P., Ho, T. K., Nguyen, N. Y., et al. (2023c). Polyethylenimine-functionalized fibroin nanoparticles as a potential oral delivery system for BCS class-IV drugs, a case study of furosemide. *J. Mater. Sci.* 58, 9660–9674. doi:10.1007/S10853-023-08640-Y

Pham, D. T., Saelim, N., Cornu, R., Béduneau, A., and Tiyaboonchai, W. (2020a). Crosslinked fibroin nanoparticles: investigations on biostability, cytotoxicity, and cellular internalization. *Pharmaceuticals* 13, 86. doi:10.3390/PH13050086

Pham, D. T., Saelim, N., and Tiyaboonchai, W. (2018). Crosslinked fibroin nanoparticles using EDC or PEI for drug delivery: physicochemical properties, crystallinity and structure. *J. Mater. Sci.* 53, 14087–14103. doi:10.1007/s10853-018-2635-3

Pham, D. T., Saelim, N., and Tiyaboonchai, W. (2019a). Alpha mangostin loaded crosslinked silk fibroin-based nanoparticles for cancer chemotherapy. *Colloids Surfaces B Biointerfaces* 181, 705–713. doi:10.1016/j.colsurfb.2019.06.011

Pham, D. T., Saelim, N., and Tiyaboonchai, W. (2020b). Paclitaxel loaded EDC-crosslinked fibroin nanoparticles: a potential approach for colon cancer treatment. *Drug Deliv. Transl. Res.* 10, 413–424. doi:10.1007/S13346-019-00682-7

Pham, D. T., Tetyczka, C., Hartl, S., Absenger-Novak, M., Fröhlich, E., Tiyaboonchai, W., et al. (2019b). Comprehensive investigations of fibroin and poly(ethylenimine) functionalized fibroin nanoparticles for ulcerative colitis treatment. *J. Drug Deliv. Sci. Technol.* 57, 101484. doi:10.1016/j.jddst.2019.101484

Pham, D. T., Thao, N. T. P., Thuy, B. T. P., Tran, V. D., Nguyen, T. Q. C., and Nguyen, N. T. (2022b). Silk fibroin hydrogel containing Sesbania sesban L. extract for rheumatoid arthritis treatment. *Drug Deliv.* 29, 882–888. doi:10.1080/10717544.2022.2050848

Pham, D. T., and Tiyaboonchai, W. (2020). Fibroin nanoparticles: a promising drug delivery system. *Drug Deliv.* 27, 431–448. doi:10.1080/10717544.2020.1736208

Prommajak, T., Kim, S. M., Pan, C. H., Kim, S. M., Surawang, S., and Rattanapanone, N. (2014). Identification of antioxidants in young mango leaves by LC-ABTS and LC-MS. *Chiang Mai Univ. J. Nat. Sci.* 13, 317–330. doi:10.12982/CMUJNS. 2014.0038

Saénz, C., Tapia, S., Chávez, J., and Robert, P. (2009). Microencapsulation by spray drying of bioactive compounds from cactus pear (Opuntia ficus-indica). *Food Chem.* 114, 616–622. doi:10.1016/j.foodchem.2008.09.095

Samanta, S., Chanda, R., Ganguli, S., Gopi Reddy, A., and Banerjee, J. (2019). Anti-diabetic activity of mango (*Mangifera indica*): a review. doi:10.15406/mojbb.2019.06.00131

Singleton, V. L., and Rossi, J. A. (1965). Colorimetry of total phenolics with phosphomolybdic-phosphotungstic acid reagents. *Am. J. Enology Vitic.* 16, 144–158. doi:10.5344/ajev.1965.16.3.144

Sirirungsee, V., Samutrtai, P., Sangthong, P., Papan, P., Leelapornpisid, P., Saenjum, C., et al. (2023). Electrosprayed nanoparticles containing mangiferin-rich extract from mango leaves for cosmeceutical application. *Nanomaterials* 13, 2931. doi:10.3390/nano13222931

Sowmya, B., Murugan, V., Jacquline Rosy, P., Saravanan, P., Rajeshkannan, R., Rajasimman, M., et al. (2023). Employing newly developed copper oxide nanoparticles for antibacterial capability from discarded Wedelia trilobata flowers. *Biomass Convers. Biorefinery*. doi:10.1007/s13399-023-03760-6

Velderrain-Rodríguez, G. R., Acevedo-Fani, A., González-Aguilar, G. A., and Martín-Belloso, O. (2019). Encapsulation and stability of a phenolic-rich extract from mango peel within water-in-oil-in-water emulsions. *J. Funct. Foods* 56, 65–73. doi:10.1016/j.jff.2019.02.045

Vepari, C., and Kaplan, D. L. (2007). Silk as a biomaterial. *Prog. Polym. Sci.* 32, 991–1007. doi:10.1016/j.progpolymsci.2007.05.013

Zhang, Y. Q., Shen, W. D., Xiang, R. L., Zhuge, L. J., Gao, W. J., and Wang, W. B. (2006). Formation of silk fibroin nanoparticles in water-miscible organic solvent and their characterization. *J. Nanoparticle Res.* 9 (5), 885–900. doi:10.1007/S11051-006-9162-X

Zhou, L., Shi, H., Li, Z., and He, C. (2020). Recent advances in complex coacervation design from macromolecular assemblies and emerging applications. *Macromol. Rapid Commun.* 41, 2000149. doi:10.1002/marc.202000149